Original Research Article

A structural investigation on polystyrene with cyclohexene mid-chain group: thermal stability and self -assembly kinetics in nonpolar and polar aprotic solutions

ABSTRACT

This study was focused on cyclohexene (CH) mid-chain functional polymer of polystyrene (PSt-CH-PSt) because of its potential application in nanotechnology and its possible usage in hierarchical structures.

Molecular and nano scale structural characterizations and thermal behavior of the powder form PSt-CH-PSt functional polymer were carried out by FTIR, SAXS, XRD and DSC methods. Solutions of PSt-CH-PSt in tetrahydrofuran and chloroform were also investigated by SAXS and FTIR.

The stable one type nano particles which have oblate core-shell shape were determined in powder form and in solution of PSt-CH-PSt. The self-assembly kinetics of the polymer indicate that the mid chain part location in oblate core shell aggregations may be controlled by polar aprotic THF and nonpolar CLF solvent effects. Exponential decreasing in oblate shell volumes of PSt-CH-PSt nano globules in THF as a function of temperature was also determined by SAXS.

Keywords: Polystyrene (PSt), Cylohexene, ATRP, Oblate Micelles, SAXS, FTIR

1. INTRODUCTION

The controlled architectures of functional polymers have attracted considerable interest in recent years, because of their possible applications as components in the synthesis of block copolymers, polymer networks, and surfactants (1,2). The functional polymers are also widely used to prepare macromonomers which are important precursors for supermolecular constructions and variety of macro polymeric architectures (3–5).

Degirmenci et al (2), previously reported that the synthesis of polystyrene (PSt) with cyclohexene (CH) mid-chain group. PSt-CH-PSt (Scheme 1) was synthesized by atom transfer radical polymerization (ATRP) of styrene (St) using 3-cyclohexene-1,1-diyldi(methylene) bis(2-bromopropanoate) as the initiator and Cu(I)/bpy as the catalyst system.

Scheme 1.

The PSt-CH-PSt polymer has active mid-chain functional alkenyl group which can cause chemically bonding and formation of self-assembled and self-organized nano aggregations in several solutions. The functional nanostructured polymers offer a great usage potential in the fields of micro system technology and efficient power generation.

Controlling of the properties of the nano formations could lead to better understanding of correlations between molecular structure, morphology, interface functionality, and the macroscopic materials. The reproducibility and long-term stability of these nano aggregations are also important to design of novel functions (6,7).

On the other hand, nanosolutions are also important to thermodynamically and kinetically controlling of the nanoparticles. The solvents can have an effect on solubility, stability and reaction rates of polymer. The knowledge of nano structural content, inner morphologies of the nano aggregations, the electron densities and assembly kinetics of the core-shell part of the nano formations in polymer solutions are very important in their potential usage in technological applications (8).

In this study tetrahydrofuran (THF) and chloroform (CLF) were selected as solvents because of their polar aprotic and nonpolar properties. THF and CLF have functional molecular groups which may cause chemical transformations and they are suitable for molecular oxidation. Therefore, these solvents are widely used to research optoelectronic properties of the polymers (9–11).

The studied polymer has electro negative charge distributions around its mid-chain (CH) part due to the presence of double bond of cyclohexene ring. With the help of the physico-chemical interactions between polymer and the solvents, the different sized nano formations may be aggregated. The molecular weights of the PSt in tetrahydrofuran and chloroform solvents are not expected to be the same because of different cross-linking of PSt part of the polymer. These solvents are also effective and kinetically include valuable information on the size, shape, morphology and the distributions of the nanoaggregations (12).

In the present work, it was firstly examined whether the PSt-CH-PSt polymer has nano aggregations or not. If it was determined, the answers were looked for about the questions related with their nano structural and molecular stabilizations. The molecular structures, nano scale shapes and inner morphologies were examined and the first step was taken to research the potential usage of PSt-CH-PSt in nano technological applications.

2. EXPERIMENTAL DETAILS

2.1 XRD

XRD pattern of the powdered polymer was obtained by a Bruker AXS, D8 Advance system by using CuK_{α} (with I=40mA and V=40kV) to investigate crystalline or amorphous structural properties of the polymer.

2.2 XRD

The thermal behaviors of the polymer were determined using differential scanning calorimetry (DSC) (Shimadzu DSC60 Model at a scanning rate of 10°C min^{-1} and temperature range from 23 to 250°C).

2.3. FTIR Spectra

FTIR spectra of solid phase polymer and polymer in chloroform (CHCl3) and tetrahydrofuran ((CH2)4O) were recorded by Perkin Elmer Spectrum One FTIR Spectrometer equipment with total reflectance diamond ATR unit at room temperature in the 4000–450 cm^{-1} range with a resolution of 4 cm^{-1} at 32 scans.

For variable-temperature measurement solid polymer were cast from 5 wt% solution in chloroform. The spectra were carried out in the temperature range between 20 and 120°C within 5°C interval by Graseby Specac Automatic Temperature controller unit. The samples were equilibrated in the cell for at least 10 min at each temperature. The region 4000–1000 cm^{-1} was used for thermal studies using CaF2. After 120°C, the samples were naturally cooled down to room temperature.

2.4. SAXS

Small-angle X-ray scattering method was utilized to further evaluate the liquid crystal systems observed by polarized microscopy. SAXS experiments were performed with Kratky compact Hecus system (Hecus X-ray systems, Graz, Austria) equipped with a linear collimation system and X-ray tube with a Cu target (λ= 1.54 Å). The generator was operated at a power of 2 kW (50 kV and 40 mA). Simultaneous measurements of SAXS and WAXS range were possible in the system with a linear-position sensitive detector used with 1024 channel resolution. Distances between channels and the sample-detector were 54 µm and 31.05 cm, respectively. SAXS measurements in solutions were also carried out in the temperature range of 23 - 50°C within 5°C interval by using an external temperature control unit.

The relative position of the SAXS peaks on the scattering vector (q) axis was used to determine the structure of the liquid crystal phases. Data for each test were acquired for 900s.

3. RESULTS AND DISCUSSION

3.1. XRD

Both of crystalline and amorphous phases can be observed in the polymers containing PSt (13). The phenyl rings cause to parallel ordering and crystalline phase while the molecular chains are responsible of the random amorphous phase. Because of these dual structural properties, the usage of PSt is preferable in design and synthesis of new polymers. XRD profile (Figure 1) of PSt-CH-PSt has Bragg peaks especially in 2θ range of 20° - 43°. These peaks are evidence of polystyrene crystalline phase (13). The broad peak in Bragg diffraction angle of 20° indicates crystallographic planes with interplanar distance of d=4.43 Å (λ= 1.54 Å). This value was determined as 4.67 Å for the crystalline form of PSt by Wecker's research group (13).

Even though, polystyrene (PSt) has polymeric nature, the structure of PSt-CH-PSt has crystalline and well regulated form. The reason of these stable crystallographic planes is the presence of planar phenyl groups which are parallel ordered respect to each other.

Figure 1.

3.2. DSC AND FTIR ANALYSIS

The DSC curve of PSt-CH-PSt is given in Figure 2. DSC curve reveals that the glass transition of the PSt-CH-PSt at 73.1 ºC.

Figure 2.

It is known that vibrational spectra of polymers may provide independent information on crystallinity, chain conformational regularity and chain stereoregularity (14,15).

FTIR spectra of powder form PSt-CH-PSt and its FTIR spectra in CHL and THF are given in Figure 3. The FTIR spectrum of PSt-CH-PSt showed absorption bands at 3026 and 2849 cm^{-1} corresponding to aromatic and aliphatic C-H stretchings respectively. The bands at 1601 and 1493 cm-1 are assigned to aromatic C=C stretchings. The out of plane C-H bending vibration band of benzene ring is seen at 758 cm^{-1} and ring bending vibration was observed at 698 cm^{-1} (16).

The band at 1735 cm^{-1} is assigned to C=O ester band in the mid point of polymer chain. The C–Br stretching vibration of the polymer is observed at 620 cm^{-1} in the FTIR spectrum.

The FTIR results of polymer in solution indicate that there are no significant shifts of the almost all band wavenumbers. Only the carbonyl band at 1735 cm^{-1} of PSt-CH-PSt shifts to 1732 cm^{-1} in solution.

Figure 3.

We also determine the phase transition temperature of PSt-CH-PSt by temperature-dependent FTIR spectroscopy. To investigate of the effect of thermal cycling on the FTIR Spectra, similar thermal cycle as used above in recording the DSC response of PSt-CH-PSt. After complete evaporation of chloroform, the FTIR spectra of cast film of PSt-CH-PSt were collected in situ during the heating process.

The C=O band at 1735 cm^{-1} is sensitive to the temperature elevation. Figure 4 shows temperature-dependent FTIR spectra of the C=O band of PSt-CH-PSt in the region from 1770 to 1700 cm^{-1}. As can be seen from Figure 4, the changes are at frequency and intensity of this band. The absorbance band position remains constant for the temperature from 20ºC to 45ºC. The band wavenumber shifts to slightly higher wavenumbers in the temperature range of 50ºC and 65ºC and significantly shifts to higher wavenumber after 70ºC. The higher band intensity was also observed at 75ºC which indicated that the polymer phase is changing.

Figure 4.

The thermal behavior of aromatic C=C bands are quite opposite to C=O band intensity variation. After 75ºC, the band intensity of the C-C-O mode at 1254 cm-1 lower than compare to the temperature range 20 - 45ºC.

Kim and co-workes (17) reported that the orientation of C-C-O moiety in polystyrene-block-poly(n-pentyl methacrylate) at lower temperatures is different from that at higher temperatures. They concluded that the orientation of this moiety was affected by the presence of PSt chains.

Therefore, we can also conclude that the conformation of this group in the PSt-CH-PSt is different in the two temperature regions.

The heating and cooling FTIR experiments of the sample showed that the sample is reversible.

3.3. SAXS

The recorded SAXS data were illustrated in Figure 5 {I(q) scattering intensities, q magnitude of scattering vector ($q = 4\pi \sin\theta/\lambda$, with 2θ being the scattering angle)}.

Figure 5

When the SAXS profiles of the sample was investigated, first observations are indicating the presence of three peaks in q= 0.17; 0.46 and 0.57$Å^{-1}$. These considered peaks are big probably occurred by the effect of high order Bragg diffractions from crystalline structure of PSt groups.

The other SAXS data (except the peaks) were used to determine the shape, size and inner morphologies of the nanoaggregations in the polymer structure. The scattering intensity [I (q)] equations of oblate core-shell model (18) were used for fitting process of the measured data to the calculated intensities. The structural model was illustrated in Figure 6 and the obtained structural parameters about the model were given in Table 1.

Figure 6.

Table 1.

SAXS analyses showed that the obtained oblate core shell shapes of the nano aggregations are stable at different temperatures in the range of 23-50°C. The related model including molecular representations and solution effects may be also understandable by using Figure 7.

Figure 7.

In the oblate core-shell model, the bigger electron densities are indicating the presence of Br atoms which have bigger electronegativity than the other atoms According to this information, it may obtain that, the tails (including Br atoms) are located in the core part of the nanoglobules in THF and in the shell part of the aggregations in CLF solutions.

When the temperature dependence of core and shell volume was investigated in the solutions, it was seen that the core volume is slightly changing (initially increasing up to of 30-35°C and then decreasing). On the other hand, the shell volume of the nanoaggregations is exponentially changing especially in THF solution (Figure 8) and these termo responsive change was defined by an empirical equation of V=A exp (-BT), (A and B are coefficients and their values were determined as 22026 $Å^3$ and 0.023 $°C^{-1}$, respectively).

Figure 8.

The studied polymer (in powder and solution forms) may be defined by nano structured and self-assembled systems. The significant results may be briefly given as follows.

i. The molecular structure of PSt-CH-PSt has stable and reversible in both of powder and two studied (THF and CLF) solution forms in the temperature range of 20-75°C.

ii. The glass transition temperature of the polymer was measured as 73.1°C.

iii. Polymer structure forms ellipsoidal core-shell aggregations in both of powder and solutions forms in nanoscale.

iv. According to the successfully determined structural model, the electron densities of the core and shell parts may be obtained and it may be also, consequently defined which molecular groups are located in these parts. As a result of this analysis, the head part (CH) is located in shell part for THF solution while CH is a corona for both of powder and CLF. So it may be briefly said that the tail part and CH part of the polymer are cross-linkable in THF and CLF solutions, respectively.

v. When the thermo response behaviors were examined for two solvents, it was obtained that the shell volume is decreasing with increasing temperature and an empirical (exponential) formula may define this changing for THF.

vi. The size of the polymer micelles is not in the expected range of 1-100 nm as nano micelles in the studied solvents. The size range of the big radius of elliptical micelles are 71.71-83.55 nm for THF and 79.39-81.80 nm for CLF. But it is also predicted that if the water percentage is increased in the solutions, the size of the aggregations will be decreased and the more compact new morphologies such as core-shell cylinders will be appeared because of polar properties of water molecules (19).

This secondary phase of the present work was also planned to take under the control of the micellar size.

4. CONCLUSION

Consequently, it may be briefly said that, the first step was taken to investigate whether this polymer may be useful to prepare micelle globules in different solvents or not. The results were positive but the nano globular formations, their morphologies and inner structures of the polymer indicate that the researches on the polymer should be developed by using the other concentrations and different additional solvents to cause more compact (smaller sized) globules, the opening and closing of the defined ellipsoidal micelles, etc. The nano carrier micelles of the PSt-CH-PSt may be developed and used in near planned technological applications especially because of their reverse micelle-forming properties and stable structures under the studied temperatures.

REFERENCES

1. Degirmenci M, Izgin O, Acikses A, Genli N. Synthesis and characterization of cyclohexene oxide functional polystyrene macromonomers by ATRP and their use in photoinitiated cationic polymerization. React Funct Polym [Internet]. 2010;70(1):28–34. Available from: http://dx.doi.org/10.1016/j.reactfunctpolym.2009.09.010

2. Degirmenci M, Acikses A, Genli N. Well-Defined Cyclohexene Oxide Mid-Chain Functional Polystyrene Macromonomer: Synthesis, Characterization and Photoinitiated

Cationic Homo- and Copolymerization. Macromol Chem Phys [Internet]. 2010;211(20):2193–200. Available from: http://doi.wiley.com/10.1002/macp.201000219

3. Hadjichristidis N, Pitsikalis M, Iatrou H, Pispas S. The Strength of the Macromonomer Strategy for Complex Macromolecular Architecture: Molecular Characterization, Properties and Applications of Polymacromonomers. Macromol Rapid Commun. 2003;24(17):979–1013.

4. Gao H, Ohno S, Matyjaszewski K. Low polydispersity star polymers via cross-linking macromonomers by ATRP. J Am Chem Soc [Internet]. 2006 Nov 29 [cited 2016 Feb 5];128(47):15111–3. Available from: http://dx.doi.org/10.1021/ja066964t

5. Boutevin B, David G, Boyer C. Telechelic oligomers and macromonomers by radical techniques. Adv Polym Sci. 2007;206(1):31–135.

6. Robeson L. Polymer Blends: A Comprechenesive Review. Robeson L, editor. Munich, Germany: Hunser; 2007.

7. Harrats C, Thomas S, Groeninckx G. Micro- and Nanostructured Multiphase Polymer Blend Systems: Phase Morphology and Interfaces. New York: Taylor & Francis; 2006.

8. Yao X, Chen D, Jiang M. Formation of PS- b -P4VP/Formic Acid Core−Shell Micelles in Chloroform with Different Core Densities. J Phys Chem B [Internet]. 2004 Apr [cited 2016 Feb 5];108(17):5225–9. Available from: http://dx.doi.org/10.1021/jp038000j

9. Heffner GW, Pearson DS. Molecular characterization of poly(3-hexylthiophene). Macromolecules [Internet]. 1991 Nov [cited 2016 Feb 5];24(23):6295–9. Available from: http://dx.doi.org/10.1021/ma00023a035

10. Huang Y, Cheng H, Han CC. Unimer–Aggregate Equilibrium to Large Scale Association of Regioregular Poly(3-hexylthiophene) in THF Solution. Macromolecules [Internet]. 2011 Jun 28 [cited 2016 Feb 5];44(12):5020–6. Available from: http://dx.doi.org/10.1021/ma200273u

11. Zagorevskii D V., Nasrullah MJ, Raghunadh V, Benicewicz BC. The effect of tetrahydrofuran as solvent on matrix-assisted laser desorption/ionization and electrospray ionization mass spectra of functional polystyrenes. Rapid Commun Mass Spectrom. 2006;20(2):178–80.

12. Davis FJ. Polymer Chemistry A Practical Approach. New York: Oxford University Press; 2004.

13. Wecker SM, Davidson T, Cohen JB. A structural study of glassy polystyrene. J Mater Sci. 1972;7(11):1249–59.

14. Koening JL. Spectroscopy of polymers. Washington DC, USA: American Chemical Society (ACS); 1992. 450 p.

15. Everall NJ, Griffiths PR, Chalmers JM, editors. Vibrational Spectroscopy of Polymers: Principles and Practice. Wiley; 2007. 586 p.

16. Smith BC. Infrared Spectral Interpretation: A Systematic Approach. Washington D. C, USA: CRC Press; 1998. 288 p.

17. Kim HJ, Kim S Bin, Kim JK, Jung YM, Ryu DY, Lavery KA, et al. Phase behavior of a weakly interacting block copolymer by temperature-dependent FTIR spectroscopy. Macromolecules. 2006;39(1):408–12.

18. Kotlarchyk M, Chen S-H. Analysis of small angle neutron scattering spectra from polydisperse interacting colloids. J Chem Phys [Internet]. 1983;79(5):2461. Available from: http://link.aip.org/link/?JCPSA6/79/2461/1%5Cnhttp://www.bayesapp.org/struct/%5Cnhttp://scitation.aip.org/content/aip/journal/jcp/79/5/10.1063/1.446055

19. Schuetz P, Greenall MJ, Bent J, Furzeland S, Atkins D, Butler MF, et al. Controlling the micellar morphology of binary PEO-PCL block copolymers in water-THF through controlled blending. Soft Matter [Internet]. 2011;7(2):749–59. Available from: http://dx.doi.org/10.1039/C0SM00938E

Table 1. Structural parameters of the nanoaggregations in powder form and solution (Tetrahydrofuran and Chloroform).

PSt-CH-PSt (Powder)									
T (℃)	Scale	Core big. rad.	Core small rad. (Å)	Oblate big rad. (Å)	Oblate small rad. (Å)	ρ core ($Å^{-2}$) $\times 10^{-5}$	ρ shell ($Å^{-2}$) $\times 10^{-6}$	ρ solvent ($Å^{-2}$)	Background (cm^{-1})

		(Å)						× 10^{-6}	
23	1.3	793.4	40.8	1152.9	294.3	10.7	9,8	9.5	219.0
25	1.3	811.4	39.0	1090.9	305.2	11.0	9.9	9.6	178.0
30	1.3	799.5	38.2	1093.1	305.5	11.1	9.8	9.5	178.3
35	1.3	803.4	37.9	1119.7	307.5	11.2	9.8	9.5	177.8
40	1.3	805.3	37.6	1119.9	307.2	11.2	9.8	9.5	181.8
45	1.3	811.4	38.9	1112.7	308.1	10.9	9.8	9.5	185.1
50	1.3	785.5	38.0	1059.7	306.3	11.1	9.8	9.6	188.2
PSt-CH-PSt (Tetrahydrofuran)									
23	0.9	699.2	533.2	820.9	540.2	3.1	9.9	9.4	192.4
25	1.0	688.7	532.5	803.8	538.4	3.0	9.9	9.4	201.5
30	1.0	710.2	534.3	829.2	538.5	2.9	10.3	9.5	176.8
35	1.0	709.2	538.3	835.5	541.9	2.8	11.0	9.4	179.2
40	1.0	711.6	535.5	825.5	538.7	2.7	11.4	9.5	175.7
45	1.0	706.6	536.0	832.1	538.9	2.7	11.7	9.4	174.8
50	1.1	763.3	124.1	717.1	748.1	1.6	12.6	9.6	552.8
PSt-CH-PSt (Chloroform)									
23	0.9	675.6	519.1	801.3	530.4	4.4	10.3	9.5	196.8
25	1.0	691.1	524.5	813.3	532.9	7.4	10.0	9.5	195.3
30	0.9	698.3	526.5	798.3	534.7	8.2	9.9	9.5	193.6
35	0.	699.9	523.	796.3	530.8	8.7	9.9	9.5	192.8

	9		1						
40	0.9	700.5	521.5	793.9	528.7	9.3	9.8	9.5	193.1
45	1.0	691.9	522.2	818.0	528.8	9.3	9.8	9.4	192.6
50	0.9	706.7	521.7	803.2	527.6	10.0	9.9	9.3	193.2

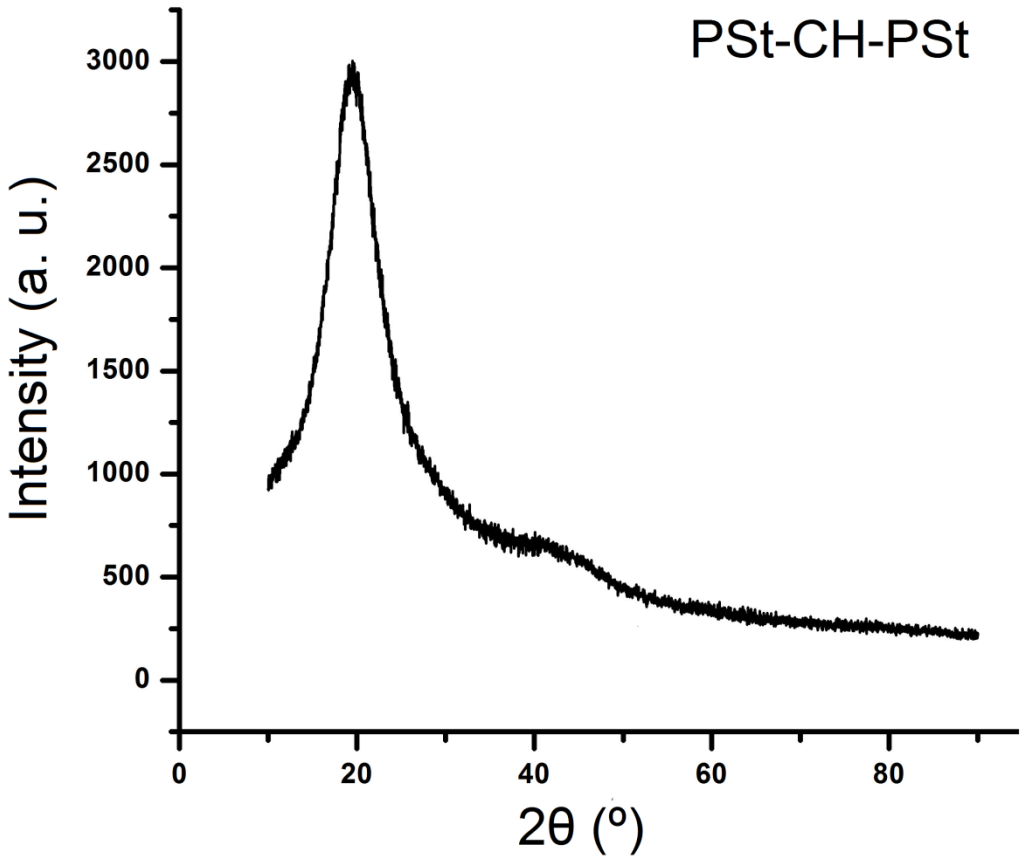

Figure 1. X-Ray Powder diffraction pattern 2θ (º) of PSt-CH-PSt polymer

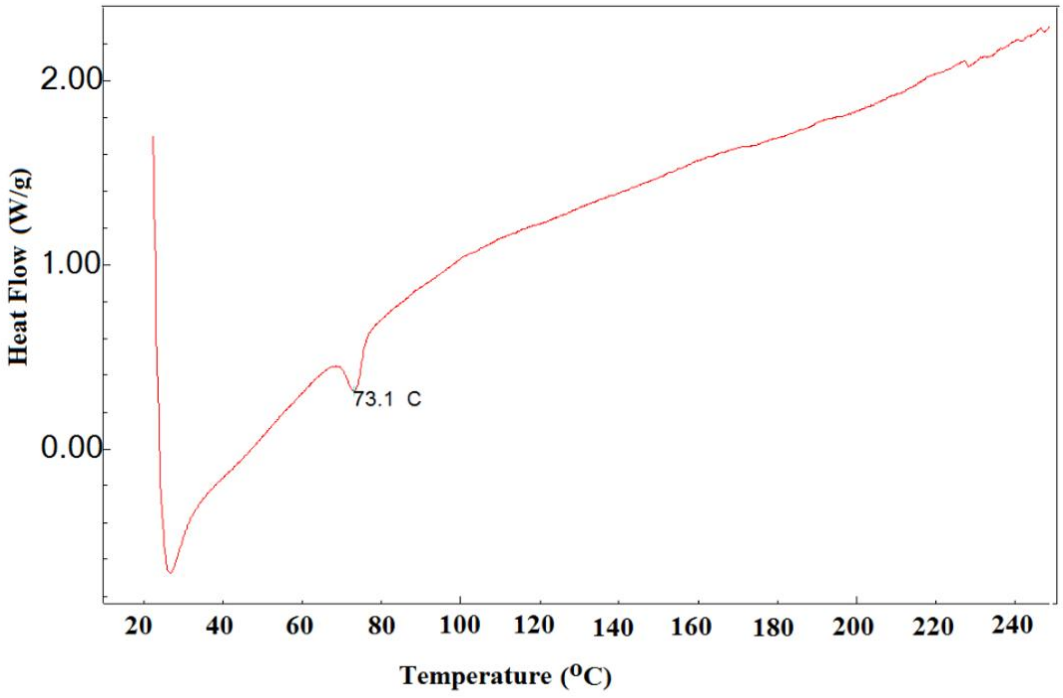

Figure 2. DSC curve of PSt-CH-PSt polymer

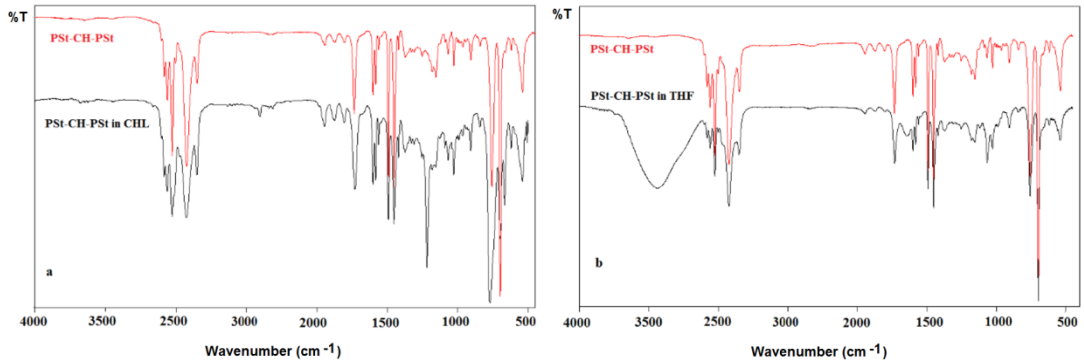

Figure 3. FTIR-ATR spectra of PSt-CH-PSt polymer in CLF (a) and THF (b). For comparison purpose FTIR spectrum of its powder form was also registered

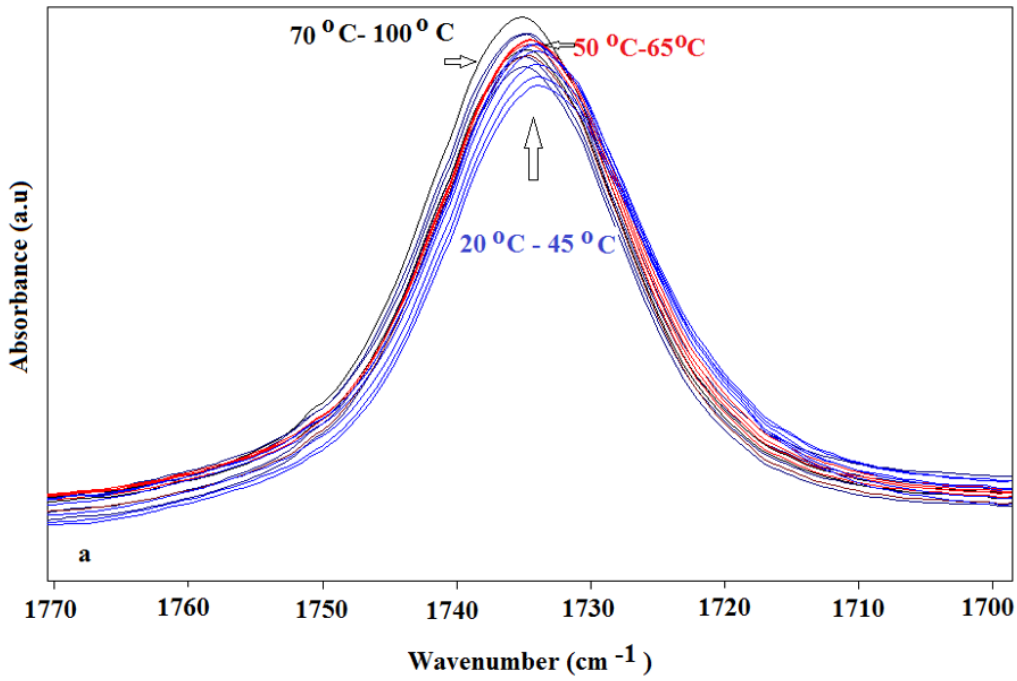

Figure 4. The thermal behavior of C=O band determined by FTIR.

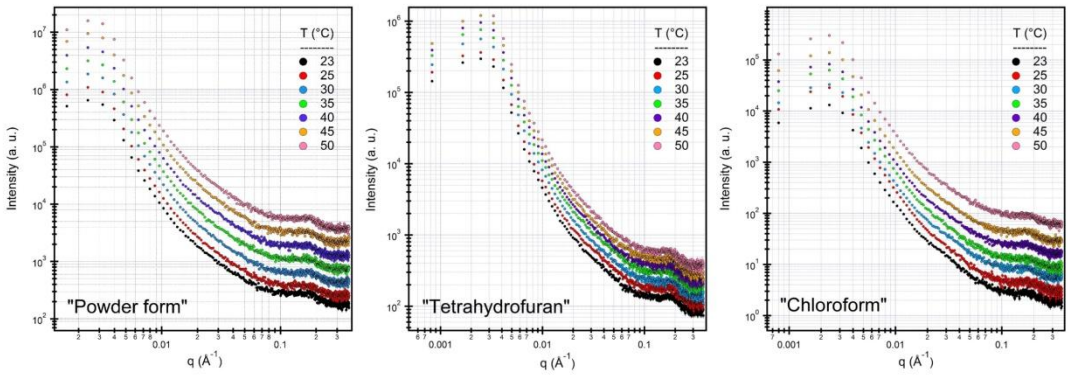

Figure 5. SAXS profiles of PSt-CH-PSt polymer as powder and in solutions.

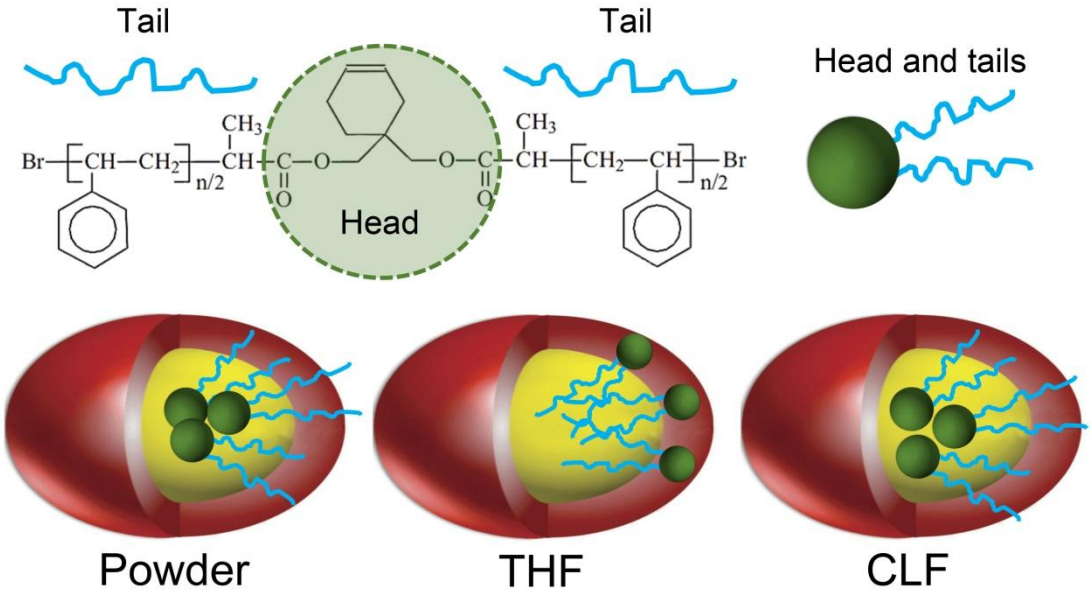

Figure 7. Inner molecular structures of the ellipsoidal core-shell shaped nanoglobules